The Effect of Pressure on Hydrogen Transfer Reactions with Quinones

Frank Wurche,[a] Wilhelm Sicking,[a] Reiner Sustmann,[a] Frank-Gerrit Klärner,*[a] and Christoph Rüchardt[b]

Abstract: The effect of pressure on the oxidation of hydroarenes **3**–**9** with 2,3-dichloro-5,6-dicyano-1,4-quinone (DDQ; **1a**) or *o*-chloranil (**10**), leading to the corresponding arenes, has been investigated. The activation volumes were determined from the pressure dependence of the rate constants of these reactions monitored by on-line UV/Vis spectroscopic measurements in an optical high-pressure cell (up to 3500 bar). The finding that they are highly negative and only moderately dependent on the solvent polarity ($\Delta V^{\neq} = -13$ to -25 in MTBE and -15 to $-29\,\text{cm}^3\text{mol}^{-1}$ in MeCN/AcOEt, 1:1) rules out the formation of ionic species in the rate-determining step and is good evidence for a hydrogen atom transfer mechanism leading to a pair of radicals in the rate-determining step, as was also suggested by kinetic measurements, studies of kinetic isotope effects, and spin-trapping experiments. The strong pressure dependence of the kinetic deuterium isotope effect for the reaction of 9,10-dihydroanthracene **5**/**5**-9,9,10,10-D_4 with DDQ (**1a**) can be attributed to a tunneling component in the hydrogen transfer. In the case of formal 1,3-dienes and enes possessing two vicinal C–H bonds, which have to be cleaved during the dehydrogenation, a pericyclic hydrogen transfer has to considered as one mechanistic alternative. The comparison of the kinetic deuterium isotope effects determined for the oxidation of tetralin **9**/**9**-1,1,4,4-D_4/**9**-2,2,3,3-D_4/**9**-D_{12} either with DDQ (**1a**) or with thymoquinone **1c** indicates that the reaction with DDQ (**1a**) proceeds in a stepwise manner through hydrogen atom transfer, analogously to the oxidations of 1,4-dihydroarenes, whereas the reaction with thymoquinone **1c** is concerted, following the course of a pericyclic hydrogen transfer. The difference in the mechanistic courses of these two reactions may be explained by the effect of the CN and Cl substituents in **1a**, which stabilize a radical intermediate better than the alkyl groups in **1c**. The mechanistic conclusions are substantiated by DFT calculations.

Keywords: DFT calculations · isotope effects · kinetics · oxidation · quinones · radicals

Introduction

Quinones are important oxidizing reagents in synthetic[1,2] and biological processes.[3] For example, the oxidation of hydroarenes by quinones such as 2,3-dichloro-5,6-dicyano-1,4-quinone (DDQ, **1a**) or *p*-chloranil (**1b**) is frequently used for the synthesis of aromatic compounds.[1,2] Five mechanisms for the quinone oxidation of hydroarenes have been proposed (Scheme 1):

1) Direct hydride transfer, leading to a pair of ions from which the observed products can be formed by proton transfer.[1,2]
2) Hydrogen atom transfer, leading to a pair of free radicals in the rate-determining step, followed by fast reactions such as disproportionation of the free radicals or single-electron transfer (SET) and subsequent proton transfer, producing the observed arene and hydroquinone.[4,5]
3) SET from the hydroarene to the quinone, followed by a proton transfer, producing the same pair of radicals as the hydrogen atom transfer, which reacts further as described under (2).[6]
4) A pericyclic ene reaction, leading to a covalently bound adduct, which is subsequently cleaved by a retro-ene reaction to yield the observed products after keto–enol tautomerization.[7]
5) Finally, a pericyclic dyotropic hydrogen transfer.[8] This is limited, however, to hydroarenes possessing two vicinal C–H bonds that can both be cleaved in the product-determining step.[9]

[a] Dr. F. Wurche, Dipl.-Ing. W. Sicking, Prof. Dr. R. Sustmann, Prof. Dr. F.-G. Klärner
Institut für Organische Chemie der Universität Duisburg-Essen
Universitätsstrasse 5, 45117 Essen (Germany)
Fax: (+49) 201-183-4252
E-mail: frank.klaerner@uni-essen.de

[b] Prof. Dr. C. Rüchardt
Institut für Organische Chemie und Biochemie
der Universität Freiburg
Albertstrasse 21, 79104 Freiburg i. Br. (Germany)

 DOI: 10.1002/chem.200305686

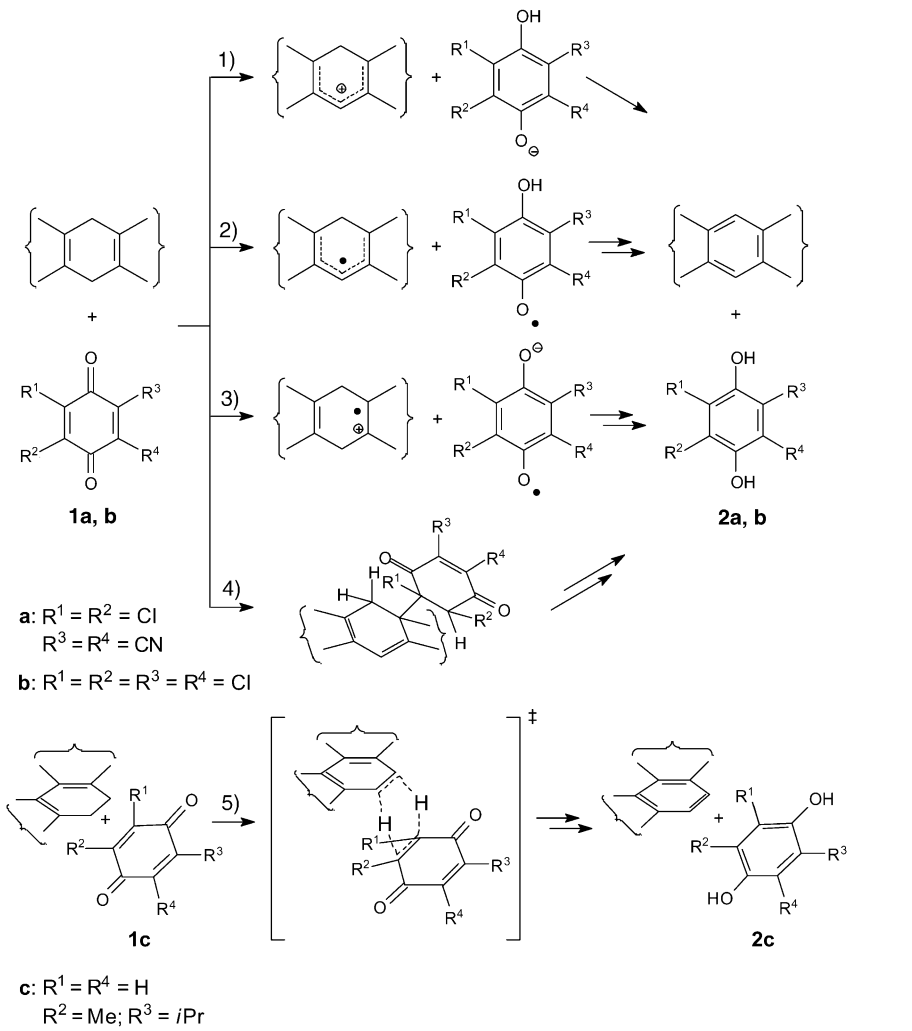

Scheme 1. Mechanistic alternatives for quinone dehydrogenation of hydroaromatic compounds: 1) direct hydride transfer, 2) hydrogen atom transfer, 3) single-electron transfer, 4) ene and retro-ene reaction, and 5) pericyclic dyotropic hydrogen transfer.

From the observations that the oxidation of hydroarenes with quinones follows second-order kinetics, that the rate of reaction is enhanced by increasing solvent polarity but only moderately, and that products of carbenium ion rearrangements are occasionally observed, Braude, Linstead, et al.[1] have proposed the direct hydride transfer (1) as the most probable mechanism. Further support for this proposal, widely accepted even today,[10] is provided by the lack of rate effects when free radical initiators or inhibitors were added. This, indeed, excludes free radical chain reactions quite safely, but certainly not a stoichiometric non-chain homolytic process as discussed for the hydrogen atom transfer (mechanism (2)).[4] The findings that the effect of solvent polarity on the rate of reaction is small[11] and comparable to the effects observed for free radical reactions[12] and that xanthene **6** reacts more rapidly than **5** with DDQ (**1a**) only by a factor of 16 at 25 °C ($\Delta\Delta G^{\neq} = 2\,\text{kcal}\,\text{mol}^{-1}$)[4] is good evidence in favor of the hydrogen atom transfer and against the direct hydride transfer, in which the carbenium ions derived from **5** and **6** would have to be generated in the rate-determining step. Because of the large difference in the stabilities of these cations[13] a huge difference in the reactivity of **5** and **6** would be expected in the case of the direct hydride transfer, contrary to the experimental observations.[4] The large primary kinetic isotope effects (k_H/k_D = 8.3 and 7.85) measured for the reactions of **5**/**5**-9,9,10,10-D_4 and **6**/**6**-9,9-D_2, respectively, at 50 °C[4] indicate that the hydrogen is transferred in the rate-determining transition state and rule out a single-electron transfer in the rate-determining step preceding the proton transfer in a fast subsequent process. A distinction between a hydrogen atom transfer and a proton-coupled electron transfer, as discussed for the benzyl/toluene, methoxy/methanol, and phenoxy/phenol self-exchange reactions,[14] is not experimentally feasible, so we do not consider this possibility below. Further evidence for the hydrogen atom transfer is provided by spin-trapping experiments. In the reactions of **5** and **6** with DDQ (**1a**), intermediary radicals could be trapped by nitrosobenzene, producing the more stable radicals **12** and **13** detected by ESR spectroscopy.[4]

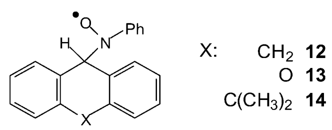

To gain further insight into the mechanism of the quinone oxidation we investigated the effects of pressure on the reactions of the hydroarenes **3**–**9** (Scheme 2) with DDQ (**1a**) and *o*-chloranil (**10**) and on the primary kinetic isotope effect k_H/k_D in the reaction of **5**/**5**-9,9,10,10-D_4 with **1a**. Compounds **1a** and **10** are reduced to **2a** and **11** in the reaction. Comparison between the kinetic isotope effects k_H/k_D in the reactions of the tetralin derivatives **9**/**9**-1,1,4,4-D_4/**9**-D_{12} either with **1a**, previously unknown and first reported here, or with thymoquinone **1c**, which have been studied by Brower et al.,[9] allows a distinction to be made between the potential mechanisms (2) and (5).

The effect of pressure on quinone dehydrogenations: determination of volumes of activation and reaction: Pressure in

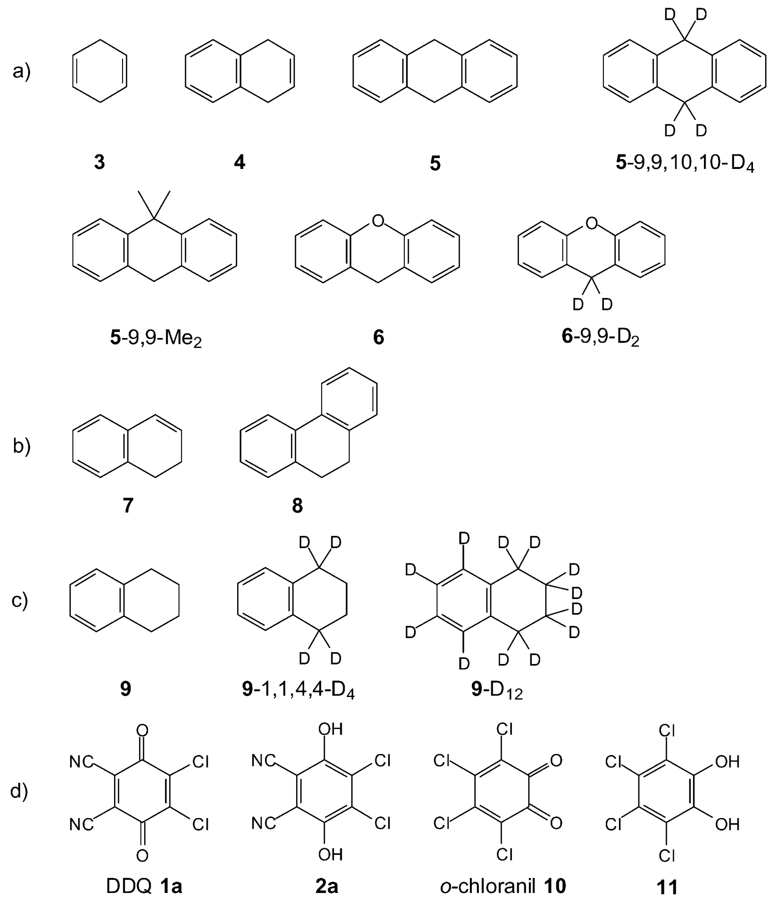

Scheme 2. The hydroaromatic compounds used as hydrogen or deuterium donors: a) formal 1,4-dienes, b) formal 1,3-dienes, c) formal enes, and d) the quinones used as oxidizing reagents and the resulting hydroquinones.

the range of 1–20 kbar influences the rate and equilibrium position of many chemical reactions.[15] Processes accompanied by a decrease in volume—such as association, ionization, and cyclization—are accelerated by pressure (volume of activation $\Delta V^{\neq} < 0$) and the equilibria are shifted toward the side of the products (volume of reaction: $\Delta V < 0$). The reverse reactions—such as homolytic dissociation, neutralization of charges, and cycloreversion—lead to an increase in volume. In these reactions, pressure induces a deceleration and a shift of equilibrium toward the side of the reactants ($\Delta V^{\neq}$, $\Delta V > 0$). The overall change in the molar volume during a reaction, as determined experimentally from the volumes of activation and of reaction, consists of the changes in the intrinsic volumes of the reacting molecules ΔV_W (V_W = van der Waals volume) and of the changes in the empty space between the molecules (void and expansion volume),[16] which is required for thermally induced motions and collisions in the liquid state. How important it is to consider the whole ensemble of molecules and not single molecules for the explanation of the pressure effect can be demonstrated in the effect of electrostriction,[17] which we also need for the explanation of the pressure effects reported here. In a heterolytic bond dissociation, the attractive interaction between the newly generated ions and the solvent molecules leads to a contraction of volume generally much larger than the expansion of volume resulting from the dissociation. Thus, the overall effect, called electrostriction, leads to negative volumes of activation and reaction.[17] In associative formation of ions—in the alkylation of pyridine derivatives (Menshutkin reaction)[18] or in the polar [2+2] cycloaddition of a vinyl ether to tetracyanoethylene (TCNE),[19] for example—both effects are volume-contracting and sum to give highly negative volumes of activation and reaction, which are strongly dependent on the solvent polarity. In nonpolar solvents the volume contraction caused by the effect of electrostriction is larger than in polar solvents. For example, the activation volume of the [2+2] cycloaddition of *n*-butyl vinyl ether to TCNE involving a zwitterionic intermediate was determined to be less negative in acetonitrile ($\Delta V^{\neq} = -23\,cm^3\,mol^{-1}$) than in CCl_4 ($\Delta V^{\neq} = -44\,cm^3\,mol^{-1}$).[19] Similar results were obtained for the alkylation of pyridine with benzyl bromide ($\Delta V^{\neq} = -29.2\,cm^3\,mol^{-1}$ in acetonitrile and $\Delta V^{\neq} = -39.1\,cm^3\,mol^{-1}$ in toluene).[18] To distinguish between the mechanistic alternatives of the quinone dehydrogenation—the direct hydride transfer leading to a pair of ions (comparable to the intermediary zwitterion in the polar [2+2] cycloaddition) and the hydrogen atom transfer leading to a pair of non-charged radicals (Scheme 1: mechanisms (1) and (2), respectively)—we determined the activation volumes of the reactions of DDQ (**1a**) with the hydroarenes **3**–**9** and of *o*-chloranil (**10**) with **5** and **6** in MTBE (*tert*-butyl methyl ether: E_T = 34.7, ε = 4.5 D) and in the more polar mixture (1:1) of acetonitrile (E_T = 45.6, ε = 35.5 D) and ethyl acetate (E_T = 38.1, ε = 6.0 D) as solvents. The low solubilities of some of the hydroarenes did not allow us to use pure acetonitrile as solvent. The rate constants k_1 of the reactions of the quinones **1a** and **10** with the hydroarenes **3**–**9** over the 1–3500 bar pressure range were determined under pseudo-first-order kinetics conditions with an excess of the hydroarene by on-line UV/Vis monitoring of the decrease in the quinone concentration in an optical 4 kbar high-pressure cell. For the example of the reaction of *o*-chloranil (**10**) with **6**, the order of the reaction was determined by measurement of the dependence of the pseudo-first-order rate constant k_{obs} on the hydroarene concentration of **6** to be, indeed, second order. Details of the determination of pressure-dependent rate constants k_1 are described in the Experimental Section. Since the slope of $\ln k_1$ against pressure (p) is not linear in the range of 1 to 3500 bar investigated here, as illustrated for the pressure dependence of the dehydrogenation of 1,4-cyclohexadiene (**3**) with DDQ (**1a**) in Figure 1, the activation volumes were determined from the slopes of these curves at $p = 0$ by use of the quadratic Equation (3) given in the Experimental Section.

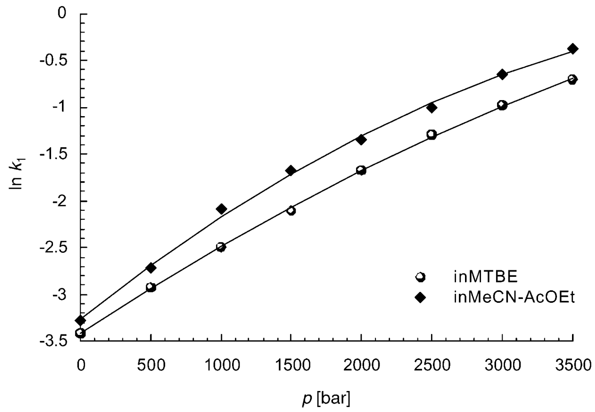

Figure 1. Pressure dependence of the second-order rate constants k_1 of the dehydrogenation of **3** with **1a** in *tert*-butyl methyl ether (MTBE) and in acetonitrile/ethyl acetate (MeCN/AcOEt) at 25.1 °C.

The activation volumes of the dehydrogenation of the hydroarenes **3**–**9** with DDQ (**1a**) or *o*-chloranil (**10**) are listed in Table 1, together with the other activation parameters enthalpy ($\Delta H^{\ddagger}$), entropy ($\Delta S^{\ddagger}$), and Gibbs enthalpy ($\Delta G^{\ddagger}$) of activation, which were taken from the literature.[20] The unknown parameters for the reaction of **5** and **6** with **10** were obtained from the temperature dependence of the rate constants at atmospheric pressure measured in this work.

The complete volume profile for the reaction between DDQ (**1a**) and 1,4-cyclohexadiene (**3**) was determined as a representative example (Figure 2). The partial molar volumes (V) of the reactants (**1a, 3**) and products (**2a**, benzene (**15**)) were obtained from density measurements in MTBE and in an MeCN/AcOEt mixture (1:1), the solvents also used for determination of the activation volumes. The reaction volume ($\Delta V = (V(\mathbf{2a})+V(\mathbf{15}))-(V(\mathbf{1a})+V(\mathbf{3}))$ and (within the scope of Eyring transition state theory) also the partial molar volume of the transition state ($V^{\ddagger} = (V(\mathbf{1a})+V(\mathbf{3})+\Delta V^{\ddagger})$ can be calculated from these partial molar volumes and the activation volume. The van der Waals volumes (V_W[22]) of the starting and transition structures involved in this reaction (defined by the space occupied by the van der Waals spheres of the atoms) were calculated from the Cartesian coordinates of the molecular structures predicted by quantum mechanical calculations (vide infra). The ratio V_W/V or $V_W^{\ddagger}/V^{\ddagger}$ is defined as the packing coefficient of a starting or transition structure(η and $\eta^{\ddagger}$) and provides information about the packing of the molecular structures in the liquid state, and hence of how much empty space is between the molecules.[16]

DFT calculations on the mechanism of hydrogen transfer: Density functional calculations (B3LYP) were performed on the mechanism of the hydrogen transfer reactions from 1,4-cyclohexadiene (**3**) to DDQ (**1a**) and *o*-chloranil (**10**). Gaussian 98[23] was used with two basis sets (6–31G* and 6–31G**), and restricted or unrestricted calculations were carried out where appropriate. Ground states and transition structures (TSs) were characterized by vibrational analysis and in each case correspond to minima or maxima (one imaginary frequency) on the potential energy surface. Table 2 displays the enthalpies (298.15 K), dipole moments, and ΔH values relative to starting materials. Two transition structures were considered in each case (Figure 3 and Figure 4), one showing an extended (TS_1) and the other one a compact structure (TS_2). For each reaction, TS_2 is lower in energy: by 1.6 kcal mol^{-1} (**1a** and 6–31G**) and 0.8 kcal mol^{-1} (**10** and 6–31G**), respectively. Similar differences, but slightly higher in absolute values, are obtained with the 6–31G* basis set. The preference for the compact structures might reflect favorable π–π interactions of the π-electrons of the electron-deficient quinone with those of 1,4-cyclohexadiene. Alternatively, it might be argued that the structure of TS_2 enables stabilizing CH–π interactions of one of the hydrogen atoms of the CH_2 group of cyclohexadiene with the π-electrons of the quinone. The closest $CH\cdots C_{sp^2}$ distance is 3.08 pm, and the angle $C{-}H\cdots C_{sp^2}$ is 149°. This arrangement is typical for CH–π interactions.[24] Another interesting feature concerns the increases in the dipole moments of the transition structures in relation to those of the starting materials. While **3** has no dipole moment, the calculated μ of **1a** (DDQ) is 4.0 D and of **10**

Table 1. Volumes of activation ($\Delta V^{\ddagger}$) and activation parameters of the dehydrogenation of hydroarenes to the corresponding arenes by DDQ (**1a**) and by *o*-chloranil (**10**) (MTBE = *tert*-butyl methyl ether, MeCN = acetonitrile, AcOEt = ethyl acetate).

Quinone	H-donor	T [°C]	$\Delta V^{\ddagger}_{MTBE}$ [cm^3 mol^{-1}]	$\Delta V^{\ddagger}_{MTBE/AcOEt}$ [cm^3 mol^{-1}]	$\Delta H^{\ddagger}$[a] [kcal mol^{-1}]	$\Delta S^{\ddagger}$[a] [E.U.]	$\Delta G^{\ddagger}_{25°C}$[a] [kcal mol^{-1}]
DDQ (**1a**)	**3**	25.1	−24.4 ± 0.2	−29.5 ± 0.5	11.7 ± 0.1	−28.2 ± 0.4	20.1 ± 0.1
	4	25.0	−24.8 ± 0.2	−28.9 ± 0.4	10.8 ± 0.1	−28.7 ± 0.7	19.4 ± 0.2
	5	25.1	−25.9 ± 0.3	−26.9 ± 0.8	11.7 ± 0.1	−28.1 ± 0.3	20.1 ± 0.1
	7	39.9	−25.3 ± 0.4	−28.4 ± 0.5	12.9 ± 1.2[b]	−29.9 ± 3.6[b]	22.6 ± 1.2[b]
	8	39.9	−25.1 ± 0.5	−29.4 ± 0.5	16.2 ± 0.8	−25.6 ± 2.4	23.8 ± 0.9
	9	64.9	–	−26.7 ± 0.4[c]	–	–	–
	5–9,9-Me_2	39.9	−20.0 ± 0.3	−22.9 ± 0.2	–	–	–
10	**5**	25.1	−16.4 ± 0.3	−18.1 ± 0.5[c]	13.3 ± 0.3[d]	−24.0 ± 1.0[d]	20.4 ± 0.3[d]
	6	25.1	−13.0 ± 0.2	−15.5 ± 0.3[c]	12.1 ± 0.3[d]	−25.6 ± 1.0[d]	19.7 ± 0.3[d]

[a] Ref.[20], solvent dioxane. [b] Ref.[21]. [c] In acetonitrile. [d] This work.

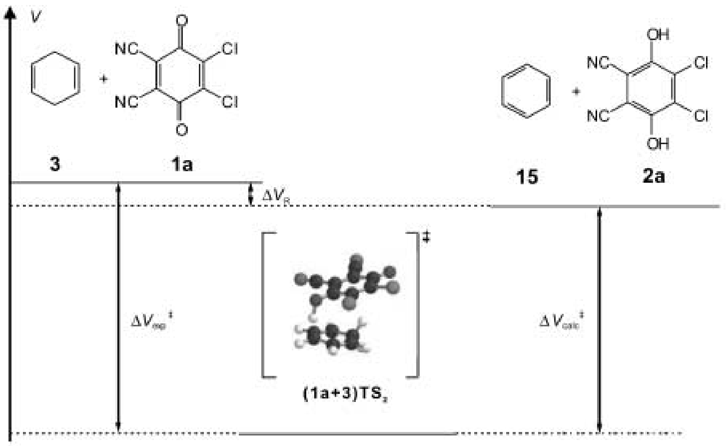

Solvent	$\Delta V_{exp}^{\ddagger}$ [a]	$\Delta V_{calcd}^{\ddagger}$	ΔV_R		3	1a	(1a + 3)TS$_2$	15	2a
tert-butyl methyl ether	–24.5	–22.3	–2.2	V_M	93.1	146.2	214.9[b]	88.7	148.4
				V_W	56.6	101.1	155.2	53.6	103.0
				η	0.608	0.692	0.723	0.604	0.694
MeCN/ AcOEt	–29.5	–26.8	–2.8	V_M	95.0	147.8	213.2[b]	89.8	150.2
				V_W	56.6	101.1	155.2	53.6	103.0
				η	0.596	0.684	0.728	0.597	0.686

[a] All volumes in $cm^3 \cdot mol^{-1}$. [b] $V^{\ddagger} = \Sigma V_{startingmaterials} + \Delta V^{\ddagger}$.

Figure 2. Volume profile[a] of the reaction between 1,4-cyclohexadiene (**3**) and DDQ (**1a**). The van der Waals volumes V_W were calculated from the Cartesian coordinates of the ground and transition structures resulting from quantum mechanical calculations by use of the MOLVOL computer program.[22]

3.4 D. Whereas the transition structures for hydrogen transfer to *o*-chloranil (**10**) show increases in μ of about 1 D ((**3**+**10**)TS$_1$ and (**3**+**10**)TS$_2$), these increases are more than 4 D ((**1a**+**3**)TS$_2$) and more than 6 D ((**1a**+**3**)TS$_1$) in the case of DDQ (**1a**). This indicates a net electron flow between the reactants, in particular in the case of the more electron-deficient DDQ. Natural population analysis (NPA) of the charge distributions for (**1a**+**3**)TS$_1$ and (**1a**+**3**)TS$_2$ indicates surpluses of negative charge on **1a** of –0.5 to –0.6 electrons and deficiencies of corresponding magnitude of electrons in **3**. If, however, the charge of +0.4 on the migrating hydrogen atom is attributed to DDQ and taken away from **3**, then the overall process does not show hydride transfer character, but, in contrast, hydrogen atom transfer character. An important property of the transition structures is the position of the transferred hydrogen atom. According to the DFT calculations the C–H bond length of the CH_2 hydrogen atoms in 1,4-cyclohexadiene is 1.10 Å, while this bond is stretched to 1.33 Å for (**3**+**10**)TS$_1$ and 1.37 Å for (**1a**+**3**)TS$_1$. The elongation of the C–H bond length is more pronounced in TS$_2$, being 1.41 Å both in (**3**+**10**)TS$_2$ and in (**1a**+**3**)TS$_2$. The OH bonds undergoing formation are 1.27 Å in (**3**+**10**)TS$_1$ and 1.22 Å in (**1a**+**3**)TS$_1$, being shorter and identical (1.19 Å) in the compact TS$_2$s. The 6–31G** basis set provides comparable, sometimes slightly smaller distances (see Figure 3 and Figure 4). The conclusion is that the hydrogen atom is midway between starting materials and products. In all the transition structures, the negative vibration corresponds to the transfer of the hydrogen atom from **3** to **1a** or **10**. Although CAS(2,2) is approximate and crude,[25] we determined the biradical characters (BRCs) of the transition structures (see Table 2). Depending on the basis set, the values range from 16 to 34%. As observed in other examples,[26] such low BRCs also yield closed-shell wave functions (S^2 = 0) when determined by unrestricted

Table 2. B3LYP DFT calculations on the mechanism of hydrogen transfer; basis sets 6–31G* (A) and 6–31G** (B).

Structure	H (298.15 K) [a.u.] A	$\Delta H^{\neq}$[a] [kcal mol^{-1}] A	μ [D] A	%BRC CAS(2,2)/6–31G* A	3_E–1_E [kcal mol^{-1}] A	H (298.15 K) [a.u.] B	$\Delta H^{\neq}$[a] [kcal mol^{-1}] B	μ [D] B	%BRC CAS(2,2)/6–31G* B	3_E–1_E [kcal mol^{-1}] B
1a	–1485.0185[b]		4.0			–1485.0185[b]		4.0		
3	–233.2897[b]		0.0			–233.3022[b]		0.0		
(**1a**+**3**)TS$_1$	–1718.2868[c]	13.4	10.6	34	8.2	–1718.3024[c]	11.5	10.4	30	8.9
(**1a**+**3**)TS$_2$	–1718.2893[c]	11.9	8.5	23	14.6	–1718.3050[c]	9.9	8.3	21	15.3
10	–2219.7395[b]		3.4			–2219.7395[b]		3.4		
(**3**+**10**)TS$_1$	–2453.0069[c]	14.0	4.7	30	7.3	–2453.0223[c]	12.2	4.7	25	8.3
(**3**+**10**)TS$_2$	–2453.0077[b]	13.5	4.9	18	19.0	–2453.0236[b]	11.4	4.9	16	19.7
16	–232.6783[c]		0.4			–232.6894[c]		0.4		
17a	–1485.6153[c]		7.3			–1485.6210[c]		7.3		
17b	–1485.6151[c]		5.0			–1485.6206[c]		5.0		
18a	–2220.3480[c]		0.8			–2220.3535[c]		0.8		
18b	–2220.3378[c]		3.3			–2220.3434[c]		3.3		

[a] Energy relative to reactants. [b] RB3LYP. [c] UB3LYP.

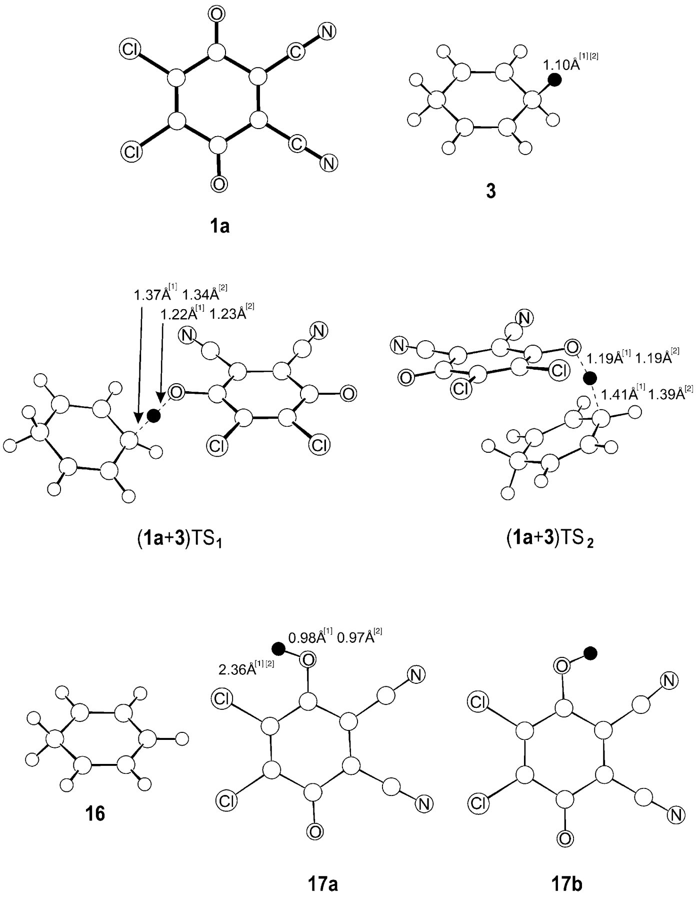

Figure 3. Calculated structures of the hydrogen transfer reaction from 1,4-cyclohexadiene (**3**) to DDQ (**1a**): [1] (U)B3LYP/6–31G*, [2] (U)B3LYP/6–31G**.

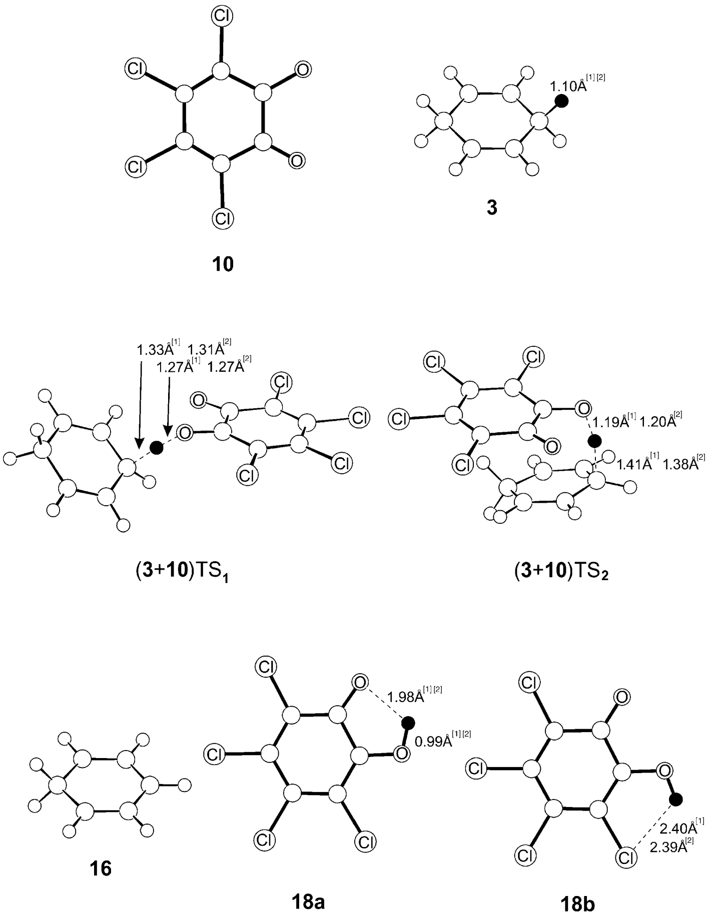

Figure 4. Calculated structures of the hydrogen transfer reaction from 1,4-cyclohexadiene (**3**) to *o*-chloranil (**10**): [1] (U)B3LYP/6–31G*. [2] (U)B3LYP/6–31G**.

DFT calculations. Further support for the closed-shell character of the transition structures is provided by the differences between the singlet and triplet biradical energies. These range from 7 to about 20 kcal mol^{-1} (Table 2), depending on basis set and the quinone under consideration. Such big differences are a measure of the closed-shell character of the systems.[26] Products of the hydrogen transfer are radicals (**16**, **17** (Figure 3), and **18** (Figure 4)). Radicals **17** and **18** may exist in two conformations with respect to the orientation of the OH bond (**a** and **b** in the formulas). While the enthalpy difference between **17a** and **17b** is marginally in favor of **17a** (0.1 kcal mol^{-1} (6–31G*) and 0.3 kcal mol^{-1} (6–31G**)), the difference between **18a** and **18b** amounts to 6.4 kcal mol^{-1} (6–31G*) or 6.3 kcal mol^{-1} (6–31G**) in favor of **18a**. This is due to a strong intramolecular OH···O hydrogen bond. If the enthalpy of reaction is calculated for **1**+**3**→**16**+**17**, values of 9.2 or 9.3 kcal mol^{-1} (6–31G*) or 6.5 or 6.8 kcal mol^{-1} (6–31G**) are obtained. The same calculation on the basis of the more stable structure **18a** for the reaction **1**+**10**→**16**+**18a** gives an enthalpy of reaction of 1.8 kcal mol^{-1} (6–31G*) or −0.8 kcal mol^{-1} (6–31G**). On the basis of the less stable structure, these values have to be corrected by about +6 kcal mol^{-1}. The reactions are therefore slightly endothermic or thermoneutral, with activation enthalpies of slightly above 10 kcal mol^{-1}. Final product formation, consisting of the disproportionation of the radicals to benzene and the corresponding hydroquinones, is a strongly exothermic process. A 6–31G* calculation, performed for the disproportionation of **16** and **17**, provides −45.6 kcal mol^{-1}. No TS could be located for this process.

Discussion

The oxidation of the hydroarenes **3**–**9** with DDQ (**1a**) or *o*-chloranil (**10**) is accelerated by pressure, indicating negative activation volumes (Table 1). Similar results have been obtained by Brower et al. for the dehydrogenation of 1,4-cyclohexadiene (**3**) and tetralin (**9**) by thymoquinone (**1c**) ($\Delta V^{\neq}$ = −33 (75 °C)[9] and −28 cm^3 mol^{-1} (175 °C)[27], respectively). The negative volumes of activation indicate an association in the rate-determining steps of these oxidations. The values of $\Delta V^{\neq}$ determined in this work, however, are only moderately dependent on the solvent polarity and even slightly more negative in the more polar medium (MeCN/AcOEt) than in MTBE, contrary to expectations for the formation of charged species. These observations are good evidence against the mechanisms of direct hydride transfer and single-electron transfer in the rate-determining step (Scheme 1 mechanisms (1) and (3)) and are further strong support for the hydrogen atom transfer (mechanism (2)). The complete volume profile shown for the reaction of **1a** with **3** in Figure 2 indicates that the partial molar volume of the transition state (calculated from the partial molar volumes of the reactants and the activation volume within the scope of the Eyring transition state theory) is the same within 1 $cm^3 mol^{-1}$ in both solvents, suggesting that there is no significant effect of electrostriction in the rate-determining transition state.

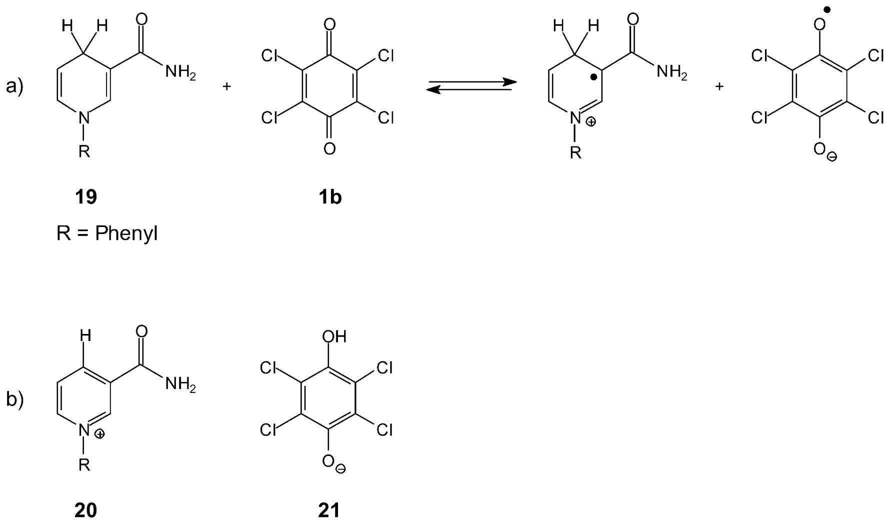

Scheme 3. a) Formation of the electron transfer complex of *N*-phenyldihydronicotinamide (**19**) with *p*-chloranil (**1b**), and b) the products of the hydrogen transfer reaction.

Experimentally determined values of activation enthalpies for hydrogen transfer are reported in Table 1 and may be compared with the DFT results shown in Table 2. The $\Delta H^{\neq}$ value of 11.7 $kcal mol^{-1}$ for the reaction of DDQ (**1a**) with 1,4-cyclohexadiene (**3**) is almost identical to the 6–31G*-calculated value for the compact (**1a**+**3**)TS_2; the 6–31G** result for the same structure is 9.9 $kcal mol^{-1}$. A compact structure is also suggested by the measurement of the highly negative activation volumes. The calculated activation enthalpy via the stretched transition structure is higher and deviates from the experimentally ascertained value more strongly. There are no experimental data for the reaction of **3** with *o*-chloranil (**10**). However, results for the reaction of 9,10-dihydroanthracene (**5**) are presented in Table 1. Compound **5** shows the same activation energy as **3** in the reaction with DDQ. Thus, it may be assumed that the dehydrogenation of **3** by **10** should provide an identical value to the reaction of **5** with **10**. The conclusion is that **10** is less reactive than DDQ. Indeed, the DFT calculations yielded a higher $\Delta H^{\neq}$ for the hydrogen transfer to *o*-chloranil, comparable to the experimentally established difference in activation energy for the reaction of **5**. The DFT results are compatible with the activation volume measurements (i.e., with a hydrogen atom transfer mechanism). There is a polar component in the mechanism, for which the increase in dipole moment in the TS of the reaction of DDQ with **3** is evidence. As this is much less pronounced for the reaction with *o*-chloranil, it may be concluded that the actual mechanism might also be dependent on the specific system. Therefore, systems in which a mechanism other than hydrogen atom transfer may be followed might exist. In the quinone oxidation of *N*-alkyl- or *N*-aryldihydronicotinamides with *p*-chloranil (**1b**), for example (Scheme 3), an intermediate—most likely the complex resulting from an electron transfer—could be detected in the UV/Vis spectrum of the mixture of *N*-phenyldihydronicotinamide (**19**) with *p*-chloranil (**1b**) in acetonitrile (λ_{max} = 448 nm).[28] At 37 °C this complex disappears within 60 min and **20** and **21** are formed as final products, as described in the Experimental Section.

The findings that the reaction of DDQ (**1a**) with 9,10-dihydroanthracene (**5**) is not significantly slower than that with 1,4-cyclohexadiene (**3**) and that the activation parameters of both reactions at 1 bar are the same rule out the ene-retro-ene mechanism (Scheme 1, mechanism 4)). In the hypothetical ene reaction of **1a** with **5**, the aromaticity of one of the benzene rings in **5** has to be given up. Therefore, this reaction should be retarded and its activation barrier should be substantially higher than that of the corresponding reaction of **1a** with **3**; comparable, for example, to the electrocyclic ring-closures of (*E*,*Z*,*E*)-2,4,6-octatriene[29] and the corresponding 4,5-benzo-anellated derivative,[30] which differ in the temperature of reaction by 100 °C and in the enthalpy of activation by $\Delta\Delta H^{\neq}$ = 3.7 $kcal mol^{-1}$.

The large primary kinetic isotope effect observed for DDQ oxidation of the hydroarenes **5** and **6** suggested an investigation of its pressure dependence. For the reaction of 9,10-dihydroanthracene **5**/**5**-9,9,10,10-D_4 with DDQ (**1a**) at 25 °C and 1 bar in MTBE the kinetic isotope effect was determined to be k_H/k_D = 10.8, decreasing to k_H/k_D = 5.0 at 3000 bar and 25 °C (Figure 5). Accordingly, the volume of

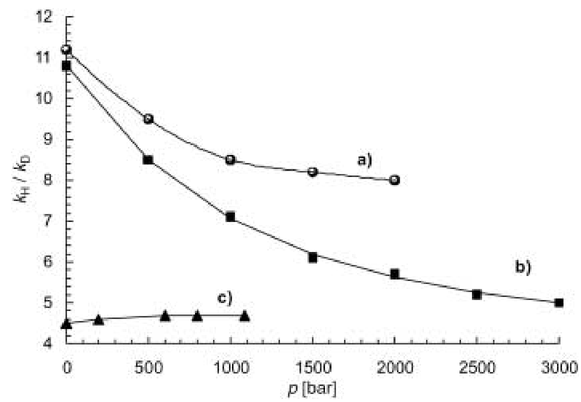

Figure 5. Effect of pressure on the kinetic isotope effect (k_H/k_D) of hydrogen transfer reactions: a) reaction of leuco crystal violet with p-chloranil in acetonitrile at 26.5 °C,[31] b) reaction of DDQ (**1a**) with **5** in MTBE at 25 °C, c) proton transfer from benzoic acid to diphenyldiazomethane at 26.5 °C.[31]

activation of the oxidation of **5**-9,9,10,10-D_4 with **1a** was calculated from the pressure dependence of the rate constants (Table 3) to be $\Delta V^{\neq} = -38.6 \pm 0.5\,cm^3 mol^{-1}$, substantially more negative than that of undeuterated **5** ($\Delta V^{\neq} = -25.9\,cm^3 mol^{-1}$). Similar results were obtained by Isaacs et al.[31] for the oxidation of leuco crystal violet with *p*-chloranil (**1b**), in which the kinetic isotope effect decreases from $k_H/k_D = 11$ at 1 bar to nearly 8 at 2000 bar ($\Delta V^{\neq} = -25$ (H) and $-35\,cm^3 mol^{-1}$ (D)). Contrary to these findings, the kinetic isotope effect on the reaction of benzoic acid and diphenyldiazomethane (proceeding by a rate-determining proton transfer) is almost pressure-independent ($k_H/k_D = 4.5$ (1 bar) and 4.7 (1090 bar) and the activation volumes for the two isotopic species are essentially identical ($\Delta V^{\neq} = -13\,cm^3 mol^{-1}$).[31] This finding indicates that the ordinary kinetic isotope effect is not significantly pressure-dependent. The strong pressure dependence of the kinetic isotope effect observed for the quinone oxidations of 9,10-dihydroanthracene **5**/**5**-9,9,10,10-D_4 and leuco crystal violet can be attributed to a tunneling component in the hydrogen transfer and can be used as a criterion for tunneling, in addition to the known kinetic indicators such as large kinetic isotope effects[32] and nonlinear Arrhenius plots[33] (large differences in the preexponential factors and activation energies for H vs. D transfer).

Table 3. Pressure-dependent second-order rate constants k_2 (in $10^{-2}\,M^{-1}s^{-1}$) for the reaction of **1a** with various hydrogen donors in *tert*-butyl methyl ether.[a]

P [kbar]	**3** k_2	**5** k_2	**5**–9,9,10,10-D_4 k_2	**5**–9,9-Me_2 k_2	**4** k_2	**7** k_2	**8** k_2
1	3.28	3.81	0.35	0.561	15.0	0.253	0.0435
500	5.37	6.73	0.80	0.76	25.2	0.417	0.0735
1000	8.2	10.7	1.52	1.10	37.5	0.627	0.112
1500	12.1	15.5	2.53	1.44	58.2	0.988	0.157
2000	18.8	23.0	4.05	1.88	82.6	1.51	0.224
2500	27.5	31.4	6.06	2.29	113	2.20	0.329
3000	37.7	43.1	8.63	2.63	144	3.15	0.425
3500	49.6	58			195		
T[°C]	25.1	25.1	25.0	39.9	25.0	39.9	39.9

[a] Initial concentrations: [**1a**] = $1.15–1.17\times10^{-3}\,M$; [**3**] = $1.87\times10^{-2}\,M$; [**5**] = $3.03\times10^{-2}\,M$; [**5**–9,9,10,10-D_4] = $3.04\times10^{-2}\,M$; [**5**–9,9-Me_2] = $1.01\times10^{-1}\,M$; [**4**] = $1.45\times10^{-2}\,M$; [**7**] = $1.04\times10^{-1}\,M$; [**8**] = $2.04\times10^{-1}\,M$.

The activation volumes ($\Delta V^{\neq}$) of the reactions of 9,10-dihydroanthracene (**5**) and xanthene (**6**) with *o*-chloranil (**10**) are substantially less negative than those of the corresponding reactions with DDQ (**1a**) (Table 1). The tendency of the solvent dependence of $\Delta V^{\neq}$ of the reactions of **10**, however, is similar to that observed for the reactions of **1a**, indicating that also in these reactions no ionic intermediates are formed in the rate-determining step and that they proceed through hydrogen atom transfer, comparably to the DDQ oxidations. In the oxidation of **5**-9,9-Me_2 and **6** with quinones **1a** or **10**, the aromatization of the intermediary radicals **22** and **23** by H atom transfer is blocked by the methyl groups or the ring oxygen atom (Scheme 4). The finding of 9,9-dimethylanthrone **26** and xanthone **27** as final products in the presence of traces of water suggests that the cations **24** and **25** are involved as intermediates in these reactions. In the reactions of **5**-9,9-Me_2 with **1a** and of **6** with **10**, spin-trapping experiments with nitrosobenzene produced the long-living nitroxide radicals **13** and **14**, which could be characterized by ESR (Experimental Section). These results are further evidence that hydrogen atom transfer also occurs in the rate-determining steps in these reactions, producing the radicals **22** and **23**, which can either be trapped by nitrosobenzene or, in the absence of a trapping reagent, can react further with excesses of the quinones to produce the cations **24** or **25**, which are converted into the final products **26** or **27** by water addition and quinone oxidation. Accordingly, oxidations of both hydroarenes either with DDQ (**1a**) or *o*-chloranil (**10**) follow the same mechanistic course. The less negative activation volumes of the *o*-chloranil oxidations may be explained by quantum mechanical calculations performed for the reactions of 1,4-cyclohexadiene (**3**) with either DDQ (**1a**) of *o*-chloranil (**10**). Accordingly, the dipole moment of the transition state

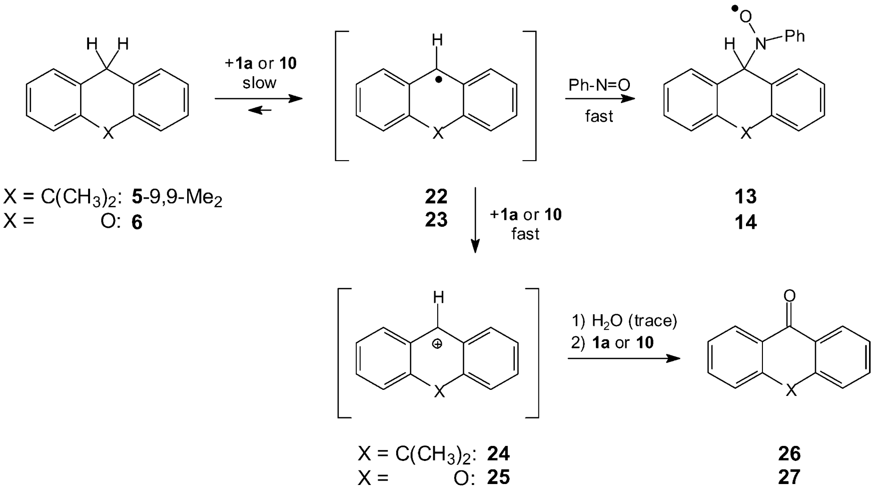

Scheme 4. The oxidation of **5**-9,9-Me_2 with **1a** and **6** with **10**, in which the aromatization by H transfer in the secondary reaction step is blocked, with spin trapping of the intermediary radicals **15** and **16** by nitrosobenzene.

of the reaction of **3** with **10** is calculated (Table 2)—with μ = 4.7 D and 4.9 D, respectively—to be substantially smaller than that of the reaction of **3** with **1a** (μ = 10.6 D and 8.5 D, respectively). Thus, the contraction of volume caused by the effects of electrostriction, and hence the activation volume, would be expected to be smaller in the reaction of **3** with **10**.

Finally, in the case of the oxidation of the formal dienes **7**, **8** and ene **9**, a pericyclic hydrogen transfer has to be considered as a potential mechanism in addition to the possibility of the hydrogen atom transfer, as already discussed in the Introduction (Scheme 1, mechanisms (2) and (4)). According to the findings obtained for pericyclic and stepwise cycloadditions (the latter involving diradical intermediates), the activation volume of the pericyclic hydrogen transfer would be expected to be more negative than that of a stepwise hydrogen atom transfer. The activation volumes of the DDQ oxidations of the formal 1,4-dienes **3–5** and the formal 1,3-dienes **7**, **8** and ene **9** do not show any significant difference (Table 1). This finding suggests the conclusion that all oxidations studied here follow the same mechanistic course. Independent support for this conclusion comes from an investigation of the kinetic isotope effect observed in the DDQ oxidation of the tetralin derivatives **9**/**9**-1,1,4,4-D_4 and **9**-D_{12}. Heesing et al.[34] have carefully studied the stereochemical course and the kinetic isotope effects for the oxidation of 1,2-dihydronaphthalene (**7**) and 1,3-cyclohexadiene (**28**) with the deuterated derivatives shown in Scheme 5 and various quinones such as **1a** and **10**. The oxidation of *cis*- and *trans*-**7**-1,2-D_2 and –**28**-5,6-D_2 proceeds with 90% and 98% *cis* stereoselectivity, respectively. These results already rule out the pericyclic hydrogen transfer as the only mechanism. Competition between a stereospecific pericyclic reaction and a non-stereoselective stepwise reaction is one mechanistic possibility. However, the observed stereoselectivity could be also explained if the subsequent hydrogen transfer were to proceed rapidly in the pair of radicals (generated in the first step) in relation to its dissociation from the solvent cage. Also, the kinetic isotope effects observed for the oxidation of the deuterated 1,2-dihydronaphthalene derivatives with **1a** and **10** (Scheme 5) do not allow clear-cut conclusions concerning the mechanism of these reactions. The finding that the reactions of both derivatives **7**-1,1-D_2 and **7**-2,2-D_2 show primary isotope effects and that the effects observed for the reactions of **7**-1,1,2,2-D_4 are larger than those found with **7**-1,1-D_2 or **7**-2,2-D_2 is in accord with a pericyclic reaction in which both C–H bonds are cleaved in the rate-determining step. The structures of two potential radical intermediates **29** and **30** (which can be obtained from **7** through H atom transfer) are both resonance-stabilized, however, so the H atom transfer from **7** may be not selective, yielding both radicals. This would also explain why the kinetic isotope effects observed for the oxidation of **7**-1,1-D_2 and **7**-2,2-D_2 with DDQ (**1a**) and *o*-chloranil (**10**) are quite different from each other. Evidently, the less reactive **10** is more selective, leading to the radical **30** preferentially, whereas the more reactive **1a** is less selective, leading to the two radicals **29** and **30** in nearly equal amounts (Scheme 6). The experimental data thus do not allow an unambiguous conclusion as to whether the quinone oxidation of 1,2-dihydronaphthalene proceeds concertedly by a pericyclic hydrogen transfer or in stepwise manner with a hydrogen atom transfer in the first step .

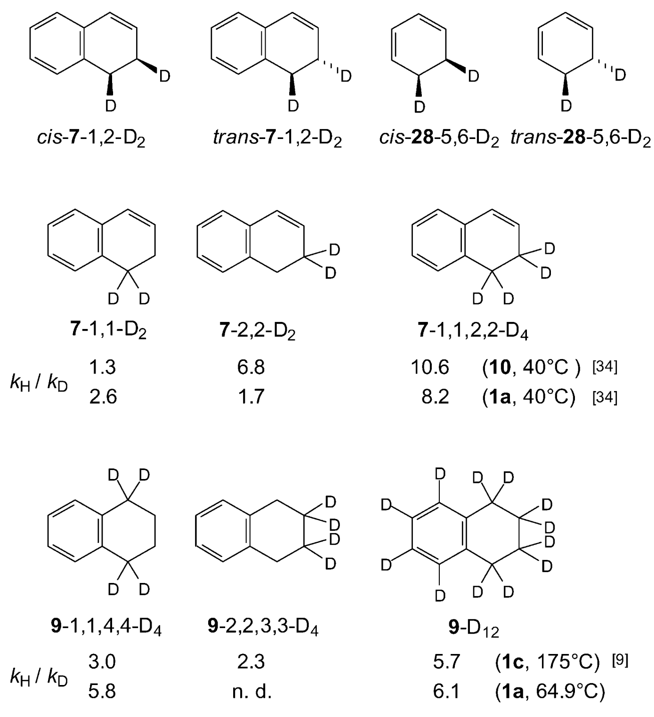

Scheme 5. Specifically deuterated 1,2-dihydronaphthalene, 1,3-cyclohexadiene, and tetralin derivatives used for investigation of the stereochemical course and the kinetic isotope effect of the quinone oxidation of formal 1,3-dienes (n. d. = not determined).

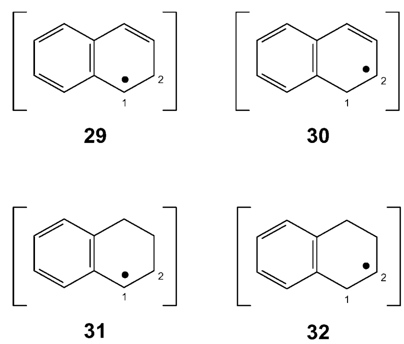

Scheme 6. Potential radical intermediates involved in the quinone oxidation of 1,2-dihydronaphthalene **7** and tetralin **9**.

In the case of the oxidation of tetralin **9** with thymoquinone **1c** on one hand and with DDQ (**1a**) on the other (leading to 1,2-dihydronaphthalene **7** as the primary isolable product), a distinction between the two mechanistic alternatives on the basis of the kinetic deuterium isotope effects was feasible.[35] The hydrogen atom transfer would be expected here to lead exclusively to the benzyl resonance-stabilized radical **31** through C^1–H bond cleavage and not to the ordinary secondary alkyl radical **32** through C^2–H bond cleavage, whereas in the pericyclic hydrogen transfer both adjacent C–H bonds have to be cleaved. Brower et al.[9]

found primary deuterium isotope effects of $k_H/k_D = 3.0$ and 2.3 for the reaction of thymoquinone **1c** with the two deuterated tetralin derivatives **9**-1,1,4,4-D_4 and **9**-2,2,3,3-D_4, respectively, and a larger value of $k_H/k_D = 5.7$ for the reaction of perdeuterated tetralin **9**-D_{12}, as would be expected for the cleavage of both C–H bonds in the rate-determining step. In contrast with these results, we found the deuterium isotope effect of the reactions of DDQ (**1a**) with **9**-1,1,4,4-D_4 and **9**-D_{12} to be nearly identical, indicating that only the C^1–H bond is broken in the rate-determining step in this reaction. This surprising finding suggests *that the reaction of tetralin* **9** *with the less reactive thymoquinone* **1c** (which requires a temperature of reaction 100 °C higher than that with DDQ (**1a**)) *proceeds via a pericyclic hydrogen transfer*, whereas *stepwise hydrogen atom transfer occurs in the reaction with* DDQ (**1a**) (Scheme 7). The different behavior of thymoquinone **1c** and DDQ (**1a**) may be explained by the different stabilities of the radicals derived from **1c** and **1a** after the hypothetical hydrogen atom transfer from **9** to **1c** or **1a**. The radical derived from **1a** should experience additional resonance stabilization by the CN and Cl,[36] substituents absent from the radical derived from **1c**. This also explains, inter alia, the high reactivity of DDQ (**1a**) in relation to all other quinones. A similar substituent effect is observed for the cyclodimerizations of 1,3-butadiene and chloroprene.[37] The [4+2] cyclodimerization of 1,3-butadiene proceeds at 120 °C predominantly in a concerted fashion, whereas in the cyclodimerization of chloroprene—occurring readily at room temperature—a stepwise [4+2] cycloaddition involving a diradical intermediate competes with concerted pathways. Evidently, the Cl substituent stabilizes the diradical intermediate, so that in the case of the chloroprene cyclodimerization the stepwise process is competitive with the concerted pathways. The different reactivity and course of reaction observed for DDQ (**1a**) and thymoquinone **1c** can be explained in terms of a substituent effect, analogously to the cyclodimerizations of 1,3-butadiene and chloroprene.

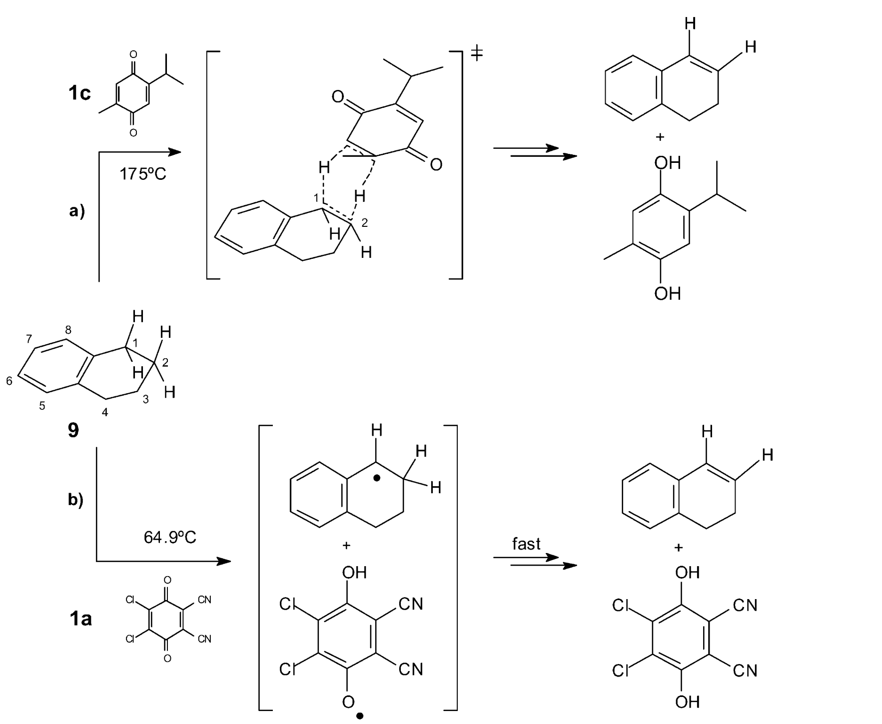

Scheme 7. Potential mechanisms of the dehydrogenation of tetralin **9** with a) thymoquinone **1c** and b) DDQ (**1a**), respectively, suggested from kinetic isotope effects.

Conclusion

The highly negative activation volumes and their moderate dependence on solvent polarity observed for oxidation of hydroarenes with DDQ (**1a**) and *o*-chloranil (**10**) are good evidence for a hydrogen atom transfer mechanism, as also suggested from kinetic measurements, studies of kinetic isotope effects, and spin-trapping experiments.[4,20] The strong pressure dependence of the kinetic deuterium isotope effect found for the reaction of 9,10-dihydroanthracene **5**/**5**-1,1,4,4-D_4 with DDQ (**1a**) can be used as a criterion for tunneling. Finally, comparison of the kinetic deuterium isotope effects determined for the oxidation of tetralin **9**/**9**-1,1,4,4-D_4/**9**-2,2,3,3-D_4/**9**-D_{12} either with DDQ (**1a**) or with thymoquinone **1c**[9] indicates that the reaction with DDQ (**1a**) proceeds in stepwise fashion through hydrogen atom transfer in the rate-determining first step, whereas the reaction with thymoquinone **1c** is concerted, following the course of a pericyclic dyotropic hydrogen transfer (Scheme 7). The difference in the mechanistic courses of these two reactions may be explained by the effect of the CN and Cl substituents in **1a**, which stabilize a radical intermediate better than the alkyl groups in **1c**. DFT calculations on the hydrogen transfer from **3** to DDQ (**1a**) and *o*-chloranil (**10**) are in agreement with these conclusions.

Experimental Section

IR: Bio-Rad FTS 135. UV: J&M Tidas FG/Cosytec/RS 422. ^{1}H NMR, ^{13}C NMR: Bruker DRX 500, Varian XL 200; the undeuterated proportion of the solvent was used as an internal standard. MS: Fisons Instruments VG ProSpec 3000. High-pressure equipment: up to 14 kbar: A. Hofer, Mülheim a. d. Ruhr; A. W. Birks, Department of Mechanical and Industrial Engineering at the Queen's University of Belfast; up to 4 kbar: Dieckers, Willich; Sitec round optical cell with sapphire windows, Zürich. GC: Hewlett Packard 5890 Series II equipped with DB1 (25 m) and OV 17 (30 m) capillary columns (d. 0.32 mm; film 0.25 µm, 2 mL min^{-1}

He flow FID); preparative GC: Varian Aerograph P 90 with WLD (Varian), column: 1.7 m, i. d. 1 cm, packed with OV17 on Volaspher A2, carrier gas: He (90 mL min^{-1}), 200 °C.

Chemicals: 9,10-Dihydroanthracene (**1a**), xanthene (**6**), DDQ, and *o*-chloranil (**10**) were obtained from Aldrich and purified by repeated crystallization from acetone/water 1:1 for **1a**, ethanol for **6**, and glacial acetic acid for DDQ and **10**, respectively, and additional sublimation under reduced pressure. Samples used for kinetic measurements had melting points in agreement with published values. 1,4-Cyclohexadiene (**3**), 1,2-dihydronaphthalene (**7**), 9,10-dihydrophenanthrene (**8**), and tetralin (**9**) (all from Aldrich) were purified by distillation under reduced pressure and stored under Argon. No significant impurities were detected by GC.

Synthesis

1,4-Dihydronaphthalene (4): Naphthalene was reduced with sodium in ethanol by the procedure described by Pajak and Brower.[9] The crude product (14.0 g), consisting of a mixture of naphthalene, 1,4-dihydronaphthalene (**4**), and 1,2-dihydronaphthalene (**7**) (12.5 %:82.3 %:4.8 % GC), was dissolved in diethyl ether (130 mL) and added dropwise to a solution of mercury(II) acetate (34.2 g) and 25 drops of glacial acetic acid in water (130 mL). After the mixture had been stirred for 24 h, the precipitated addition product was filtered off. The residue was washed with water (400 mL) and ether (250 mL). A stirred suspension of the product in petroleum ether (200 mL) was heated under reflux for four hours. After filtration the product was dried under reduced pressure to give 25.5 g. To recover **4**, hydrochloric acid (30 %, 350 mL) was added to the stirred mixture of the addition product (25.5 g) in dichloromethane (400 mL), and the mixture was stirred at room temperature for two hours. The precipitated colorless solid was removed by filtration. The aqueous phase was extracted with three portions (150 mL) of diethyl ether. The combined organic layers were washed with saturated aqueous $NaHCO_3$ (200 mL) and water (200 mL) and dried ($MgSO_4$). After evaporation of the solvents in vacuo, the yellow solid was purified by column chromatography (150 g silica gel, dichloromethane) and distillation in vacuo (25 mbar) to give pure **4** (5.1 g, m.p. 26 °C, ref.[38] m.p. 26–27 °C). GC analysis: 98.5 % of **4** and 1.5 % of naphthalene. ^1H NMR (200 MHz; $CDCl_3$): $\delta = 3.38$ (s, 4H; H-1, H-4); 5.90 (s, 2H; H-2, H-3); 7.05–7.25 ppm (m, 4H; H-Ar).

9,9-Dimethylanthrone (26): This compound was obtained by methylation of anthrone with methyl iodide as described by Herberg.[39] The crude product was purified by column chromatography (silica gel, cyclohexane/dichloromethane 2:1, yield: 12 %). m.p. = 101 °C; ^1H NMR (200 MHz; $CDCl_3$): $\delta = 1.74$ (s, 6H; $-CH_3$), 7.42 (td, $^3J = 7.5$ Hz, $^4J = 1.3$ Hz, 2H; H-3,6), 7.64 (td, $^3J = 7.5$ Hz, $^4J = 1.3$ Hz, 2H; H-2,7), 7.69 (dd, $^3J = 7.7$ Hz, $^4J = 1.4$ Hz, 2H; H-1,8), 8.36 ppm (dd, $^3J = 7.9$ Hz, $^4J = 1.5$ Hz, 2H; H-4,5); IR (KBr): $\tilde{\nu} = 1656$ (s) (C=O), 1597 cm^{-1} (s) (ArC=C).

9,9-Dimethyl-9,10-dihydroanthracene (7): Sublimed $AlCl_3$ (8.2 g, 61.3 mmol) was dissolved at 0 °C in diethyl ether (20 mL). After the addition of $LiAlH_4$ (1.2 g, 31.1 mmol), a solution of **26** (3.9 g, 17.5 mmol) in diethyl ether (30 mL) was added, and the reaction mixture was heated under reflux for 20 minutes. After cooling to room temperature, the green colored reaction mixture was quenched with water. The water layer was extracted three times with diethyl ether, the combined organic layers were dried over $MgSO_4$, and the solvent was removed in vacuo. The crude product was purified by column chromatography (silica gel, CCl_4) and recrystallized twice from ethanol at 5 °C to give **7** (1.0 g, 27 %). m.p. 49 °C; ^1H NMR (500 MHz; $CDCl_3$): $\delta = 1.64$ (s, 6H; $-CH_3$), 4.11 (s, 4H; H-10), 7.21–7.56 ppm (m, 8H; H−Ar); ^{13}C NMR (126 MHz; $CDCl_3$): $\delta = 28.8$ ($-CH_3$), 35.8 (C-10), 39.2 (C-9), 124.1 (C-1), 125.8, 126.4 (C-2,3), 127.8 (C-4), 135.6 (C-4a), 144.9 ppm (C-8a).

9,10-Dihydroanthracene-9,9,10,10-[D_4] (5-9,9,10,10-D_4) and xanthene-9,9-[D_2] (6-9,9-D_2): These were prepared by catalytic hydrogen/deuterium exchange in [D_1]ethanol/sodium ethoxide as described by Gerst and Rüchardt.[40]

a) 5–9,9,10,10-D_4: M.p. 106 °C, yield: 97 %. The degree of deuteration in **5**–9,9,10,10-D_4 was determined from the intensities (I) of the ^1H NMR signals of the deuterated **6** corrected by means of the intensities measured for the corresponding signals of the undeuterated **5** at $\delta = 3.94$–3.96 (m, H_2–9, 10, $I = 0.0359$), 7.20–7.22 (m, H-1, 4, 5, 8, $I = 1.0000$), 7.29–7.32 ppm (m, H-2, 3, 6, 7, $I = 0.9881$). From these intensities the content of deuterium at C-9, 10 was calculated to be 96.4 % (estimated error 2 %). Exact mass spectroscopic analysis of the content of deuterium in **6** was not feasible because of hydrogen/deuterium exchange occurring during measurement at 20 eV.

b) 6–9,9-D_2: m.p. 101 °C, yield: 73 %. The degree of deuteration in **6**-9,9-D_2 was determined in the same way as described for **5**-9,9,10,10-D_4: $\delta = 4.05$ (s, H_2–9, $I = 0.0336$), 7.02–7.07 (m, H-1, 3, 6, 8, $I = 1.0000$), 7.17–7.23 ppm (m, H-2, 4, 5, 7, $I = 0.9826$). From these intensities the content of deuterium at C-9 was calculated to be 96.6 % (estimated error 2 %).

1,2,3,4-Tetrahydronaphthalene-1,1,4,4-[D_4] (9–1,1,4,4-D_4): This compound was prepared by repetitive treatment of **9** with NaH in [D_6]DMSO by the method described by Bergman et al.[41] The product was purified by distillation under reduced pressure and preparative GC ($t_R = 10$ min). The degree of deuteration in **9**-1,1,4,4-D_4 was determined in the same way as described for **5**-9,9,10,10-D_4: $\delta = 1.52$ (s, H-2, 3, $I = 1.9861$), 2.56 (s, H-1, 4, $I = 0.0670$), 6.94–6.96 (m, H-5, 8, $I = 1.000$), 7.01–7.03 ppm (m, H-6, 7, $I = 1.0067$). From these intensities the content of deuterium at C-1, 4 was calculated to be 96.7 % (estimated error 2 %).

1,2,3,4-Tetrahydronaphthalene-1,1,2,2,3,3,4,4,5,6,7,8-[D_{12}] (9-D_{12}): This compound was prepared according to the synthesis of 1,2,3,4-tetrahydronaphthalene from naphthalene as described by Blum et al.[42] A mixture of $RhCl_3 \cdot 3H_2O$ (0.1 g), Aliquat-336 (methyltridecylammonium chloride, 0.22 g), D_2O (10 mL), and 1,2-dichloroethane (5 mL) was vigorously shaken in a Paar hydrogenation apparatus at 30 °C under a deuterium pressure of 1 bar for 60 min. After addition of a solution of [D_8]naphthalene (Aldrich, 5.0 g, 98 % D) in 1,2-dichloroethane (10 mL), the mixture was shaken for an additional 72 h under a deuterium pressure of 1 bar at 30 °C. The reaction mixture was extracted twice with 20 mL portions of 1,2-dichloroethane, and the combined organic layers were washed twice with 50 mL portions of water and dried over $MgSO_4$. After distillation under reduced pressure, the product was further purified by preparative GC ($t_R = 10$ min). The degree of deuteration in **9**-D_{12} was determined from the intensities (I) of the ^1H NMR signals of the deuterated **9**-D_{12} (0.327 M in [D_6]benzene) relative to the intensities of the signals of the internal standard dioxane (0.520 M). $\delta = 1.49$ (s, H-2, 3, $I = 0.3270$), 2.53 (s, H-1, 4, $I = 0.3183$), 3.35 (dioxane, $I = 8.000$), 6.95 (m, H-6, 7, $I = 0.0511$), 7.03 (m, H-6, 7, $I = 0.1006$). From these intensities the content of deuterium at C-1, 4 was calculated to be 87.9 %, at C-2, 3 87.6 %, C-5, 8 95.8 %, and at C-6, 7 91.7 % (estimated error 2 %).

Kinetic measurements: The rate constants of the oxidation of the hydroaromatic compounds **3–9** with DDQ (**1a**) and *o*-chloranil (**10**) were determined by UV/Vis spectroscopy under pseudo-first-order conditions with at least 16-fold molar excess of the hydroaromatic compound. The conversion of **1a** to DDQ-H_2 (**2a**) during the reaction with the hydroaromatic compounds could be monitored by the decreases in the UV/Vis absorptions of **1a** and **10**, respectively, at wavelengths of $\lambda = 400$ nm and $\lambda = 450$ nm, at which **2a** or 1,2,3,4-tetrachloro-5,6-dihydroxybenzene (**11**) do not absorb light, as illustrated for **1a** and **2a** in Figure 6.

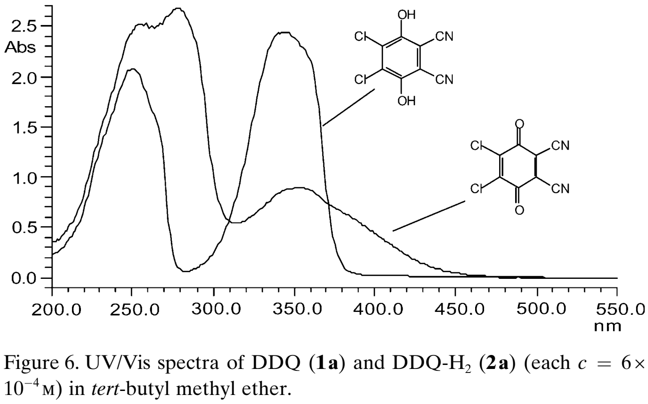

Figure 6. UV/Vis spectra of DDQ (**1a**) and DDQ-H_2 (**2a**) (each $c = 6 \times 10^{-4}$ M) in *tert*-butyl methyl ether.

Equation (1) was used to calculate pseudo-first-order rate constants k_{obs} and the bimolecular rate constant k_2, from k_{obs} and the initial concentration of the hydroarene, which can be assumed to be constant due to the large excess of the hydroarene.

$$\ln(A/A_0) = k_{obs}t \text{ with } k_{obs} = k_2[\text{H-donor}] \quad (1)$$

In the reaction of 1,4-cyclohexadiene (**3**) with DDQ (**1a**) the decrease in the absorption A at three different wavelengths (400, 415, and 430 nm) with time was used to calculate the pseudo-first-order rate constants, by use of Equation (1), as $k_{obs} = (1.548 \pm 0.005)\,s^{-1}$ at 400 nm, $(1.540 \pm 0.004)\,s^{-1}$ at 415 nm, and $(1.544 \pm 0.004)\,s^{-1}$ at 430 nm ($[\mathbf{3}] = 1.87 \times 10^{-2}$ M, $[\mathbf{1a}] = 1.16 \times 10^{-3}$ M), which agree within limits of experimental error. All other rate constants of the reactions of **3**–**9** with **1a** were calculated only from the decrease in the absorption at 430 nm and those with **10** at 437 nm.

The reaction order was determined by measurement of k_{obs} at various H-donor concentrations. From a plot of $\log k_{obs}$ versus log [H-donor] according to Equation (2), a slope of one indicates that the reaction order is one in terms of the H-donor following second order kinetics, as shown for the reaction of xanthene (**6**) with **10** as example (Figure 7).

$$\log k_{obs} = \log k_2 + x \log [\text{H-donor}] \quad (2)$$

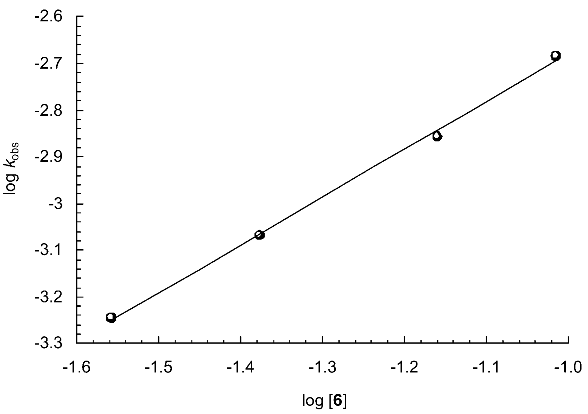

Figure 7. Plot of $\log k_{obs}$ versus log [**6**] for the reaction of xanthene (**6**) with *o*-chloranil (**10**). The slope was determined to be $x = 1.03 \pm 0.03$.

The pressure dependence of the rate constants was measured in a high-pressure optical cell ($p_{max} = 4$ kbar, SITEC) which was connected to a 4 kbar vessel, heated by an external oil bath thermostated to ±0.2 °C, and pressurized by a motor-driven press (Dieckers). To follow the time dependence of the reactions of the quinones **1a** and **10** with one of the hydrocarbons **3**–**9** and of **1b** with *N*-phenyldihydronicotinamide (**19**) at elevated pressures and temperatures, pre-thermostated solutions of the quinone and the hydrocarbon were mixed and immediately transferred into the high-pressure optical cell, which was connected to a diode-array UV/Vis spectrometer by a fiber optic link. With this equipment, the schematic cross section of which is depicted in Figure 8, the decrease in the quinone concentration could be monitored on-line continuously, as illustrated in Figure 9 for the reaction of **3** with **1a** in *tert*-butyl methyl ether at 25.1 °C and 500 bar.

For the reaction of **1b** with **19** at 37.0 °C, the time-dependent decrease in the absorption of the electron transfer complex at 448 nm is depicted in Figure 10. The first spectrum was obtained one minute after mixing of the reaction solutions of **1b** ($c = 1.05 \times 10^{-3}$ M) and **19** ($c = 2.21 \times 10^{-2}$ M) in acetonitrile in the high-pressure optical cell. From the time dependence of the decrease in the UV/Vis absorption at 37 °C and 1 bar, the pseudo-first-order rate constant was ascertained to be $k_{obs} = (3.9 \pm 0.2) \times 10^{-2}\,s^{-1}$. Because of the high sensitivity of the reaction to the presence of small amounts of oxygen in the high-pressure optical cell it was not possible also to determine the pressure dependence of the pseudo-first-order rate constants of the oxidation reaction with the required accuracy to obtain the volume of activation of the reaction.

For kinetic measurements at atmospheric pressure, a thermostated tandem quartz cell, which allowed thermostating of the separate solutions of the reactants, was used. The tandem quartz cell was connected to a diode-array UV/Vis spectrometer by a fiber optic link. The temperature of the reaction solution, both in the high-pressure cell and in the tandem quartz cell, was checked by a calibrated resistance thermometer PT-100.

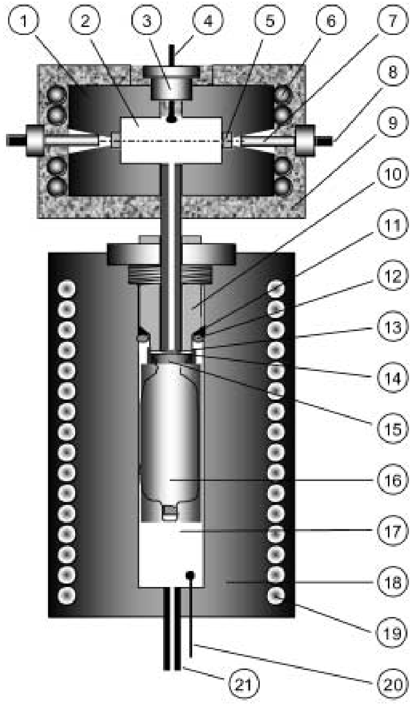

Figure 8. Schematic view of the high-pressure optical cell with pressure vessel: 1) high-pressure optical cell, 2) volume 2.2 mL, optical path 14 mm, 3) lid, 4) thermocouple, 5) sapphire windows, optical width = 6 mm, 6) heating system filled with water, 7) quartz lenses, 8) optical fiber link to the UV/Vis spectrometer, 9) heating insulation, 10) enclosed volume, 11) antiextrusion ring (Cu/Be alloy), 12) O-ring, 13) nut, 14) PTFE seal, 15) coupling for the PTFE tube, 16) PTFE tube with reaction mixture, 17) hydraulic liquid: isooctane/decalin (1:1), 18) pressure vessel ($p_{max} = 7$ kbar, volume = 25 mL), 19) heating system, filled with silicon oil, 20) thermocouple, and 21) connection to the motor-driven press, which keeps the pressure constant (±1 bar) during the experiment.

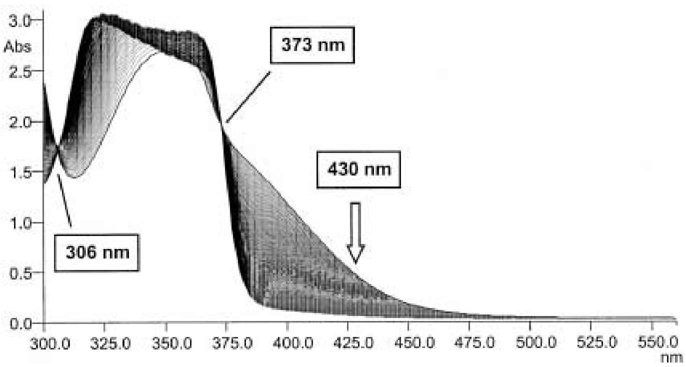

Figure 9. Array of 290 UV/Vis spectra of the reaction of DDQ (**1a**) ($c = 1.15 \times 10^{-3}$ M) with 1,4-cyclohexadiene (**3**; $c = 1.89 \times 10^{-2}$ M) in *tert*-butyl methyl ether at 25.1 °C and 500 bar.

Since the slope of the plot of $\ln k_2$ against pressure p is not linear in the 1–3500 bar range investigated here (Figure 11), the volumes of activation ($\Delta V^{\neq}$) were determined from the pressure dependence of the rate constants k_2 at a constant temperature T by use of the quadratic Equation (3).

$$\ln k_p = a + bp + cp^2 \text{ and } \Delta V^{\neq} = \Delta V_0^{\neq} = -bRT \quad (3)$$

Results are listed in Table 3, Table 4, Table 5, and Table 6

ESR spin-trapping: For the spin-trapping experiments, solutions of H-donor, quinone, and nitrosobenzene in benzene were prepared (2.0×

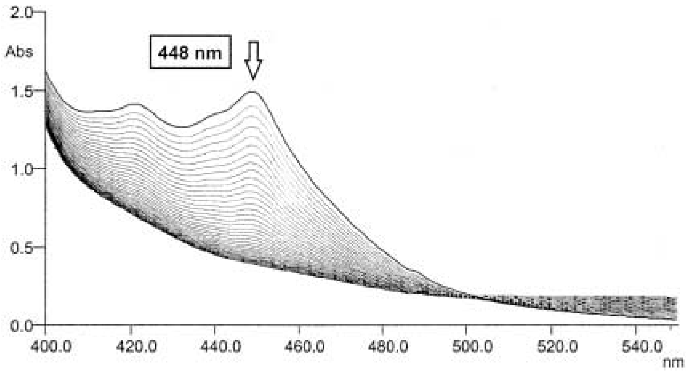

Figure 10. Array of UV/Vis spectra of the reaction of *N*-phenyldihydronicotinamide (**19**; $c = 2.21\times10^{-2}$ M) with *p*-chloranil (**1b**; $c = 1.05\times10^{-3}$ M) in acetonitrile at 37.0 °C.

Table 5. Pressure-dependent second-order rate constants k_2 (in 10^{-2} M^{-1} s^{-1}) for the reactions of **10** with **5** and **6** in *tert*-butyl methyl ether (MTBE) and acetonitrile (MeCN).[a]

p [kbar]	$\mathbf{5}_{MTBE}$ k_2	$\mathbf{5}_{MeCN}$ k_2	$\mathbf{6}_{MTBE}$ k_2	$\mathbf{6}_{MeCN}$ k_2
1	0.67	0.40	2.36	1.87
500	0.98	0.52	3.17	2.47
1000	1.26	0.76	3.94	3.53
1500	1.69	1.01	4.86	4.31
2000	2.09	1.39	6.32	5.95
2500	2.58	1.80	7.37	7.42
3000	–	2.60	9.40	9.84
3500	3.22	–	10.9	11.8
T [°C]	25.1	25.1	25.2	25.2

[a] Initial concentrations: [**10**] = 1.05×10^{-3} M; [**5**] = 9.73×10^{-2} M; [**6**] = 2.21×10^{-2} M.

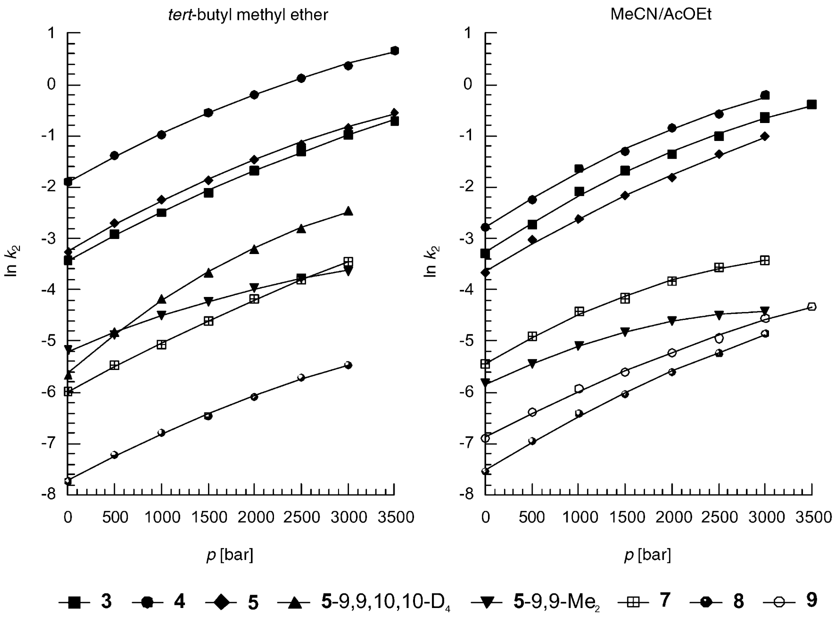

Figure 11. Pressure dependence of the rate constants k_2 of the oxidation of the hydroarenes **3–9** with **1a** in *tert*-butyl methyl ether (left) and in MeCN/AcOEt (right).

10^{-1} M **5**–9,9-Me$_2$, 7.8×10^{-2} M **1a**, and 7.8×10^{-2} M nitrosobenzene for trapping of the 9,9-dimethyl-9-hydroanthranyl radical (**22**), and 1.9×10^{-1} M **6**, 7.8×10^{-1} M **10**, and 7.8×10^{-1} M nitrosobenzene for trapping of the xanthyl radical (**23**)). Equal aliquots were mixed and degassed by use of several freeze-pump-thaw cycles. The spectra of the spin adducts were recorded at room temperature immediately after mixing. Without the addition of the quinones, but under otherwise identical conditions, no ESR spectrum was observed. For results see Table 7 and Figure 12.

Molar volumes: For each substance, the densities of solutions of seven different concentrations were determined. Measurements were performed in a temperature range from 20 to 50 °C in steps of 5 °C. For each temperature, the value of ϕ_V (apparent molar volume of a substance at a given concentrations) was calculated by using Equation (4), with c [mol L^{-1}] = concentration of the solution, M [g mol^{-1}] = molar mass of the solute, d [g cm^{-3}] = density of the solution, and d_0 [g cm^{-3}] = density of the pure solvent.

$$\phi = \frac{M}{d_0} - \frac{1000}{c}\frac{d-d_0}{d_0} \tag{4}$$

The partial molar volume (V) is calculated by linear extrapolation of ϕ_V to a concentration $c = 0$ [Eq. (5)].

$$V = \lim_{c\to0}\phi_v \tag{5}$$

The van der Waals volumes V_W of **1a** and **3** were calculated by use of the MOLVOL[22] computer program with the van der Waals radii of hydrogen (1.17 Å), carbon (1.8 Å), nitrogen (1.8 Å), oxygen (1.53 Å), and chlorine (1.8 Å).

The packing coefficients of the starting and the transition structures, η and η$^{\neq}$, were calculated by using Equations (6) and (7).

$$\eta = V_w/V \tag{6}$$

$$\eta^{\neq} = V^{\neq}_W \tag{7}$$

Table 4. Pressure-dependent second-order rate constants k_2 (in 10^{-2} M^{-1} s^{-1}) for the reaction of **1a** with various hydrogen donors in MeCN/AcOEt.[a]

P [kbar]	**3** k_2	**5** k_2	**5**–9,9,Me$_2$ k_2	**10** k_2	**7** k_2	**8** k_2	**9**[b] k_2
1	3.76	2.52	0.293	6.25	0.428	0.053	0.101
500	6.6	4.86	0.428	10.7	0.732	0.096	0.169
1000	12.4	7.21	0.61	19.4	1.19	0.164	0.264
1500	18.6	11.6	0.80	27.3	1.55	0.239	0.371
2000	25.7	16.2	1.00	43.0	2.16	0.364	0.533
2500	36.4	25.9	1.12	55.9	2.84	0.529	0.711
3000	52.6	36.2	1.21	80.9	3.26	0.773	1.05
3500	68.6						1.32
T [°C]	25.1	25.1	39.9	25.0	39.9	39.9	64.9

[a] Initial concentrations: [**1a**] = 1.15–1.17×10^{-3} M; [**3**] = 1.87×10^{-2} M; [**5**] = 3.03×10^{-2} M; [**5**–9,9-Me$_2$] = 1.01×10^{-1} M; [**4**] = 1.43×10^{-2} M; [**7**] = 1.04×10^{-1} M; [**8**] = 2.04×10^{-1} M; [**9**] = 4.59×10^{-1} M. [b] In pure acetonitrile.

Acknowledgement

This work was supported by the Deutsche Forschungsgemeinschaft and the Fonds der Chemischen Industrie.

Table 6. Temperature-dependent second-order rate constants k_2 (in $10^{-2}\,\text{M}^{-1}\,\text{s}^{-1}$) for the reactions of **10** with **5** and **6** in *tert*-butyl methyl ether.[a]

T [°C]	**5** k_2	**6** k_2
20.2	0.427	1.44
25.9	0.731	2.38
35.7	1.44	4.44
43.4	2.45	7.32
49.4	4.06	10.7

[a] Initial concentrations: [**10**] = 1.05×10^{-3} M; [**5**] = 9.72×10^{-2} M; and [**6**] = 2.33×10^{-2} M.

Table 7. Comparison of the coupling constants a of the spin adducts **12**, **13**, and **14**.

Coupling	**14** [G]	**12** [G][43]	**13** [G][43]
a_N	10.45	10.92	10.91
$a_{o\text{-}H}$	2.61	2.70	2.66
$a_{m\text{-}H}$	0.90	0.98	0.95
$a_{p\text{-}H}$	2.61	2.70	2.66
$a_{\beta\text{-}H}$	0.90	0.98	0.95
g factor	2.0056	2.056	2.0057

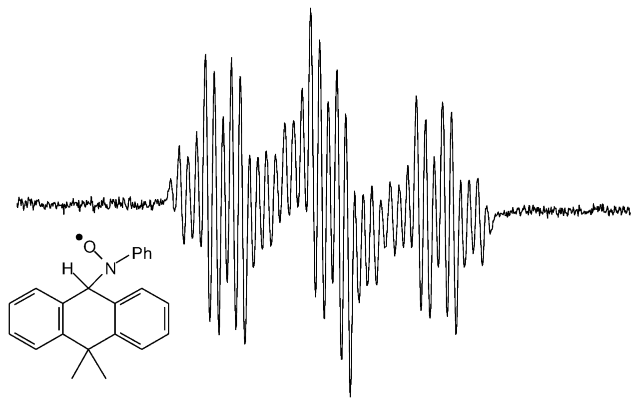

14

Figure 12. ESR spectrum of the spin adduct of the 9,9-dimethyl-9-hydroanthranyl radical to nitrosobenzene. Sweep-width 80 Gauss; microwave frequency 9.417 GHz; centerfield 3355 Gauss; modulation 0.08 Gauss.

[1] E. A. Braude, R. P. Linstead, *J. Chem. Soc.* **1954**, *3*, 3544–3547; E. A. Braude, L. M. Jackman, R. P. Linstead, *J. Chem. Soc.* **1954**, *3*, 3548–3574; J. R. Barnard, L. M. Jackman, *J. Chem. Soc.* **1960**, 3110–3115; E. A. Braude, L. M. Jackman, R. P. Linstead, J. S. Shannon, *J. Chem. Soc.* **1960**, 3116–3122; E. A. Braude, L. M. Jackman, R. P. Linstead, G. Lowe, *J. Chem. Soc.* **1960**, 3123–3138; A. M. Creighton, L. M. Jackman, *J. Chem. Soc.* **1960**, 3138–3147; L. M. Jackman, *Adv. Org. Chem.* **1960**, 329–366.

[2] H.-D. Becker, A. B. Turner, in *The Chemistry of the Quinoid Compounds, Vol. II* (Eds.: S. Patai, Z. Rappoport), Wiley, New York, **1988**, 1351–1384.

[3] L. Stryer, *Biochemistry*, W. H. Freeman, New York, **2002**; D. Voet, J. D. Voet, *Biochemistry*, Wiley, New York, **1995**.

[4] C. Höfler, C. Rüchardt, *Liebigs. Ann. Recl.* **1996**, 183–188.

[5] C. Rüchardt, M. Gerst, J. Ebenhoch, *Angew. Chem.* **1997**, *109*, 1474–1498; *Angew. Chem. Int. Ed. Engl.* **1997**, *36*, 1407–1430.

[6] Z. M. Hashish, I. M. Hoodless, *Can. J. Chem.* **1976**, *54*, 2261–2265.

[7] B. M. Jacobson, *J. Am. Chem. Soc.* **1980**, *102*, 886–887.

[8] L. A. Paquette, M. A. Kesselmayer, R. D. Rogers, *J. Am. Chem. Soc.* **1990**, *112*, 284–291; L. A. Paquette, G. A. O'Doherty, R. D. Rogers, *J. Am. Chem. Soc.* **1991**, *113*, 7761–7762; W. Grimme, K. Pohl, J. Wortmann, D. Frowein, *Liebigs Ann. Chem.* **1996**, 1905–1916.

[9] J. Pajak, K. R. Brower, *J. Org. Chem.* **1985**, *50*, 2210–2216.

[10] J. March, M. B. Smith, *March's Advanced Organic Chemistry*, 5th ed., Wiley, New York, **2001**, Chapter 19.

[11] The rate of the dehydrogenation of 9,10-dihydroanthracene **5** with DDQ (**1a**) is enhanced by the change of the solvent from dioxane (E_T = 36.0 kcal mol^{-1}, ε = 2.9 D) to acetonitrile (E_T = 45.6 kcal mol^{-1}, ε = 3.9 D) only by a factor of 3.6 (Ref. [4]).

[12] K. U. Ingold, *Pure Appl. Chem.* **1997**, *69*, 241–244; C. Reichardt, *Solvents and Solvent Effects in Organic Chemistry*, Wiley-VCH, Weinheim, **2003**, chapter 5.3.4.

[13] H. Mayr, M. Patz, *Angew. Chem.* **1994**, *106*, 990–1010; *Angew. Chem. Int. Ed. Engl.* **1994**, *33*, 934–958.

[14] J. M. Mayer, D. A. Hrovat, J. L. Thomas, W. T. Borden, *J. Am. Chem. Soc.* **2002**, *124*, 11142–11147.

[15] Monographs: R. van Eldik, F.-G. Klärner, *High Pressure Chemistry*, Wiley-VCH, Weinheim, **2002**; W. B. Holzapfel, N. S. Isaacs, *High-Pressure Techniques in Chemistry and Physics*, Oxford University Press, New York, **1997**; R. van Eldik, C. D. Hubbard, *Chemistry under Extreme and Non-Classic Conditions*, Wiley, New York, **1997**; K. Matsumoto, R. M. Acheson, *Organic Synthesis at High Pressure*, Wiley, New York, **1991**; W. J. le Noble, *Organic High Pressure Chemistry*, Elsevier, Amsterdam, **1988**; N. S. Isaacs, *Liquid Phase High Pressure Chemistry*, Wiley, Chichester, **1981**; Reviews: F. Wurche, F.-G. Klärner in *High Pressure Chemistry* (Eds.: R. van Eldik, F.-G. Klärner), Wiley-VCH, Weinheim, **2002**, 41–96; F.-G. Klärner, F. Wurche, *J. Prakt. Chem.* **2000**, *342*, 609–636; A. Drljaca, C. D. Hubbard, R. van Eldik, T. Asano, M. V. Basilevsky, W. J. le Noble, *Chem. Rev.* **1998**, *98*, 2167–2289; K. Matsumoto, M. Kaneko, H. Katsura, N. Nayashi, T. Uchida, R. M. Acheson, *Heterocycles* **1998**, *47*, 1135–1177; F.-G. Klärner, *Chem. Unserer Zeit* **1989**, *23*, 53–63; R. van Eldik, T. Asano, W. J. le Noble, *Chem. Rev.* **1989**, *89*, 549–688; W. J. le Noble, *Chem. Unserer Zeit* **1983**, *17*, 152–162; T. Asano, W. J. le Noble, *Chem. Rev.* **1978**, *78*, 407–489.

[16] T. Asano, W. J. le Noble, *Rev. Phys. Chem. Jpn.* **1973**, *43*, 82–91.

[17] W. J. le Noble, H. Kelm, *Angew. Chem.* **1980**, *102*, 841–856; *Angew. Chem. Int. Ed. Engl.* **1980**, *19*, 841.

[18] Y. Kondo, M. Onishi, N. Tokura, *Bull. Chem. Soc. Jpn.* **1972**, *45*, 3579; Y. Kondo, M. Shinzawa, N. Tokura, *Bull. Chem. Soc. Jpn.* **1977**, *50*, 713.

[19] J. Jouanne, H. Kelm, R. Huisgen, *J. Am. Chem. Soc.* **1979**, *101*, 151.

[20] C. Höfler, Ph.D. Dissertation, Universität Freiburg, **1997**.

[21] R. Paukstat, M. Brock, A. Heesing, *Chem. Ber.* **1985**, *118*, 2579–2593.

[22] The Van der Waals volumes V_W can be calculated by the computer program MOLVOL: U. Artschwager-Perl, Ph.D. Dissertation, Ruhr-Universität Bochum, **1989**. This program uses the Cartesian coordinates of a molecular structure resulting from a force-field or quantum mechanical calculation and can be obtained on request.

[23] Gaussian 98 (Revision A.7), M. J. Frisch, G. W. Trucks, H. B. Schlegel, G. E. Scuseria, M. A. Robb, J. R. Cheeseman, V. G. Zakrzewski, J. A. Montgomery Jr., R. E. Stratmann, J. C. Burant, S. Dapprich, J. M. Millam, A. D. Daniels, K. N. Kudin, M. C. Strain, O. Farkas, J. Tomasi, V. Barone, M. Cossi, R. Cammi, B. Mennucci, C. Pomelli, C. Adamo, S. Clifford, J. Ochterski, G. A. Petersson, P. Y. Ayala, Q. Cui, K. Morokuma, D. K. Malick, A. D. Rabuck, K. Raghavachari, J. B. Foresman, J. Cioslowski, J. V. Ortiz, B. B. Stefanov, G. Liu, A. Liashenko, P. Piskorz, I. Komaromi, R. Gomperts, R. L. Martin, D. J. Fox, T. Keith, M. A. Al-Laham, C. Y. Peng, A. Nanayakkara, C. Gonzalez, M. Challacombe, P. M. W. Gill, B. G. Johnson, W. Chen, M. W. Wong, J. L. Andres, M. Head-Gordon, E. S. Replogle, J. A. Pople, Gaussian, Inc., Pittsburgh, PA, **1998**.

[24] M. Nishio, *The CH/π Interaction*, 1st ed., Wiley-VCH, New York, **1998**.

[25] F. Jensen, *Introduction to Computational Chemistry*, Wiley, New York, **1999**.

[26] R. Sustmann, W. Sicking, R. Huisgen, *J. Am. Chem. Soc.* **2003**, 125, 14425–14434.

[27] K. R. Brower, *J. Org. Chem.* **1982**, *47*, 1889–1893.

[28] A. Sewing, Diploma Thesis, Universität Freiburg, **1997**.

[29] E. N. Marvell, G. Caple, B. Schatz, W. Pippin, *Tetrahedron* **1973**, *29*, 3781.
[30] H. Heimgartner, H.-J. Hansen, H. Schmidt, *Helv. Chim. Acta* **1972**, *55*, 1385.
[31] N. S. Isaacs, K. Javaid, E. Rannala, *J. Chem. Soc. Perkin Trans. 2* **1978**, 709 – 711.
[32] L. Melander, W. H. Saunders, *Reaction Rates of Isotopic Molecules*, Wiley, New York **1980**.
[33] G. Brunton, D. Griller, L. R. C. Barclay, K. U. Ingold, *J. Am. Chem. Soc.* **1976**, *98*, 6803 – 6811.
[34] M. Brock, H. Hintze, A. Heesing, *Chem. Ber.* **1986**, *119*, 3727 – 3736.
[35] The activation volumes of both reactions are highly negative ($\Delta V^{\neq} = -28$ (reaction of **9** with **1c** at 175 °C) and $-26.7\ cm^3 mol^{-1}$ (reaction of **9** with **1a** at 64.9 °C in MeCN/AcOEt), but the comparison of these data does not provide further insight into the mechanism. Since the two values were determined at quite different temperatures, the temperature dependence of the activation volume cannot be neglected here (See: B. S. El'yanov, E. M. Gonikberg, *J. Chem. Soc. Faraday Trans. 1* **1979**, *75*, 172 – 191; B. S. El'Yanov, E. M. Vasylvitskaya, *Rev. Phys. Chem. Jpn.* **1980**, *50*, 169 – 184). Furthermore, the size of the activation volume may also depend on the quinone structure, as found for DDQ (**1a**) and *o*-chloranil (**10**).
[36] J. J. Brocks, H.-D. Beckhaus, A. L. J. Beckwith, C. Rüchardt, *J. Org. Chem.* **1999**, *64*, 1935 – 1943.
[37] F.-G. Klärner, B. Krawczyk, V. Ruster, U. K. Deiters, *J. Am. Chem. Soc.* **1994**, *116*, 7646 – 7657.
[38] R. Huisgen, G. Seidl, *Chem. Ber.* **1963**, *96*, 2730 – 2739.
[39] C. Herberg, H. D. Beckhaus, C. Rüchardt, *Chem. Ber.* **1994**, *127*, 2065 – 2072.
[40] M. Gerst, C. Rüchardt, *Tetrahedron Lett.* **1993**, *34*, 7733 – 7736.
[41] P. B. Comita, M. R. Berman, C. B. Moore, R. G. Bergman, *J. Phys. Chem.* **1981**, *85*, 3266 – 3276.
[42] J. Blum, I. Amer, A. Zoran, Y. Sasson, *Tetrahedron Lett.* **1983**, *24*, 4139 – 4142.
[43] S. Terabe, R. Konaka, *J. Chem. Soc. Perkin Trans. 2* **1972**, 2163 – 2172.

Received: November 5, 2003

Published online: April 14, 2004

